

MODELING OF PROCESS INDUCED DEFORMATIONS OF COMPOSITE SHELL STRUCTURES

Göran Fernlund¹, Karl Nelson², and Anoush Poursartip¹

¹Metals and Materials Engineering, The University of British Columbia, Vancouver, Canada

²Boeing Phantom Works, Seattle, USA

ABSTRACT

This paper presents an engineering approach to the prediction of process-induced deformations of three-dimensional composite shell structures, using a two-dimensional special purpose finite element process code and a standard three-dimensional finite element structural code. The approach avoids the need to develop a full three-dimensional process code, significantly reducing the computational effort but still retaining much of the detail required for accurate analysis. The concept of the approach is presented together with an experimental and numerical example demonstrating the validity of the approach. Comparison between measurements and model predictions shows that the variation of flange spring-in along the length of a composite rib with end caps can be accurately predicted using this technique.

KEY WORDS: Dimensional Control, Spring-in, Process Modelling, Finite Element Analysis, 3D structures

1. INTRODUCTION

With faster computers and increased understanding of the fundamentals of composites processing, computer simulations of manufacturing processes are gaining ground in industry. There are several models for the simulation of processing of polymeric composite materials presented in the literature, e.g., [1-8]. Many of these models were developed with a focus on the fundamental science rather than for the purpose of simulation of processes in an industrial setting. However, COMPRO [9,10] is a finite element based composite structure process model that was developed with substantial input from The Boeing Company to ensure that it includes many industrially relevant effects.

COMPRO has been used to simulate processes on the Boeing 747, 767, and 777 aircraft. Much of the work has focused on dimensional control; especially process induced warpage and spring-in. Recently it was used to simulate the processing of the Boeing 767 raked wing front spar and to calculate the appropriate compensation of the tool for flange spring-in [11,12].

Although COMPRO is a two-dimensional code and all real structures are three-dimensional (3D), the effect of the third dimension is often mainly geometric and does not have a significant

effect on the residual stress build-up in the other dimensions. This means that the residual stress build-up during processing and the effect of these stresses on the final shape of a 3D structure can be separated using a sub-structure and transfer approach [13], as shown in Figure 1. The concept is to divide the structure of interest into substructures that are sectioned in two perpendicular directions and modeled using high mesh density 2D process models to capture the important phenomena causing residual stress build-up. The resulting deformations of the 2D process models are then transferred to a simple 3D shell model where the equivalent forces and stiffness, that give the same overall deformations as the 2D models, are calculated. The shell models of different representative substructures are then assembled to calculate the resulting deformations and reaction forces of the entire structure. If local stresses are required, the resulting deformations of the shell model can be transferred back to the 2D models where the local stresses are calculated.

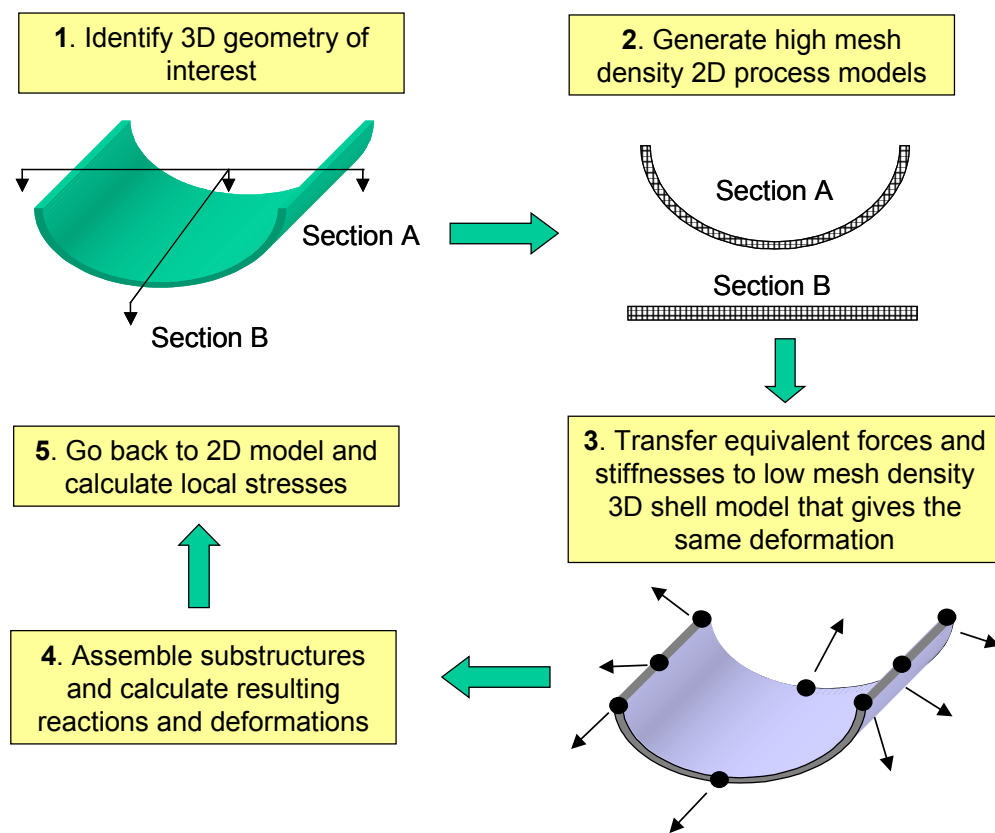


Figure 1. Schematic of sub-structuring and transfer approach.

The transfer of equivalent forces and stiffnesses from the 2D model to the 3D model will depend on the type of finite element used. The 2D process model COMPRO time-steps through the cure cycle and calculates nodal forces and element properties in each time-step. These properties can be transferred to the 3D model incrementally at each time-step or they can be added up and transferred at the end of the cure cycle. The former approach is more general and allows modelling of mechanical interaction between the part and the surroundings in full 3D during cure. An example of a phenomenon that needs to be modeled in this way is tool-part interaction. To model tool-part interaction, the 3D model should have one layer of shell elements

representing the part, one layer of shell elements representing the tool, and one layer of elements representing the tool-part interface.

2. MEASUREMENTS

To test and validate the transfer approach, the spring-in of five nominally identical carbon/epoxy ribs was studied. The rib consists of eight layers of AS4/977-3 woven carbon/epoxy prepreg (0°/45°/45°/45°)_s, and were manufactured by Boeing St. Louis. The rib is a 'box' with one side open and is processed on a positive aluminum tool (Figure 2).

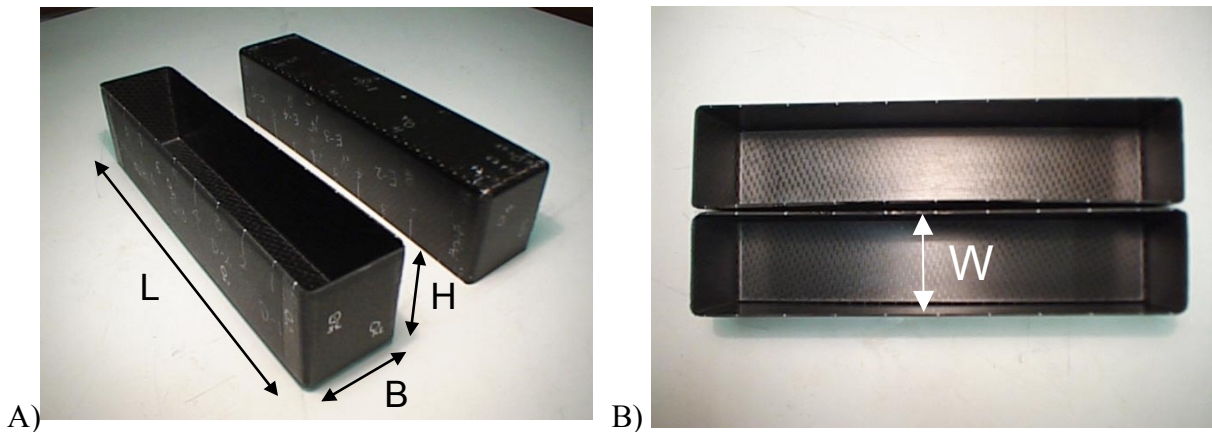


Figure 2. A) General view of ribs, B) Top view of ribs. Approximate dimensions: web width (B) 67.8 mm, flange height (H) 77.6 mm, and length (L) 310 mm.

Because of flange spring-in after cure and the stiffening effect of the ends, the flange-to-flange distance (W) is not the same as before cure. Furthermore, it is varying along the length of the rib. To examine this phenomenon in more detail, the rib geometry was measured after cure, both as a whole structure and after sectioning along the length of the rib.

2.1 Measurements Before Sectioning Five ribs were measured and the ribs were divided into 11 stations for measurement purposes. Station 0 and 10 were marked 10 mm from each edge and the rest of the stations were uniformly spaced, 31 mm apart. The flange-to-flange distance (W) was measured on the inner mould surface of the part with a digital hand caliper (Figure 3A). The distance was measured 10 times at each station and the average distance was calculated. Figure 3B shows a schematic of the measured flange spring-in, δ , of the rib before sectioning. The varying flange spring-in along the length can also be seen in Figure 2B by noting the gap between the flanges of the two ribs.

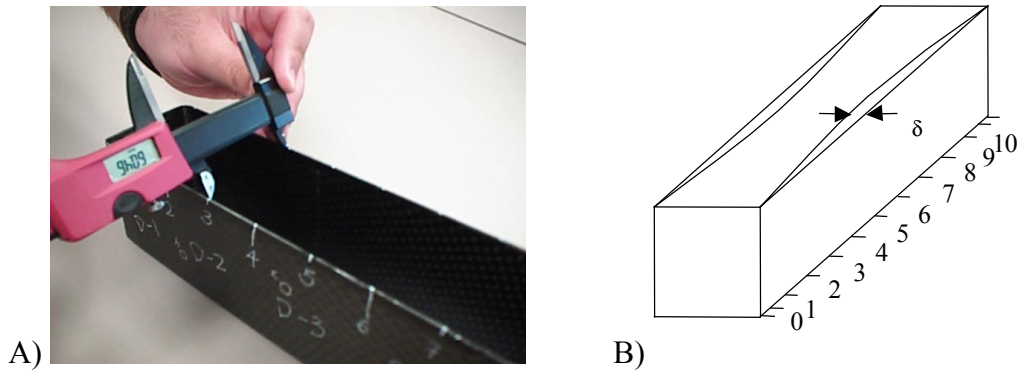


Figure 3. A) Measurement of flange-to-flange distance (W) with a digital caliper, B) Schematic of flange spring-in, δ , of the rib before sectioning

To test the hypothesis that the flange spring-in is uniform along the length of the rib if the constraint of the ends are removed, the rib was cut into sections and the flange-to-flange distance (W) was measured again.

2.2 Measurements After Sectioning The five ribs were cut in the transverse direction at stations 1, 3, 5, 7, and 9 (Figure 3B) and the two end pieces were cut in half in the longitudinal direction, see Figure 4A. Figure 4B shows the geometry and spring-in definitions of the sections.

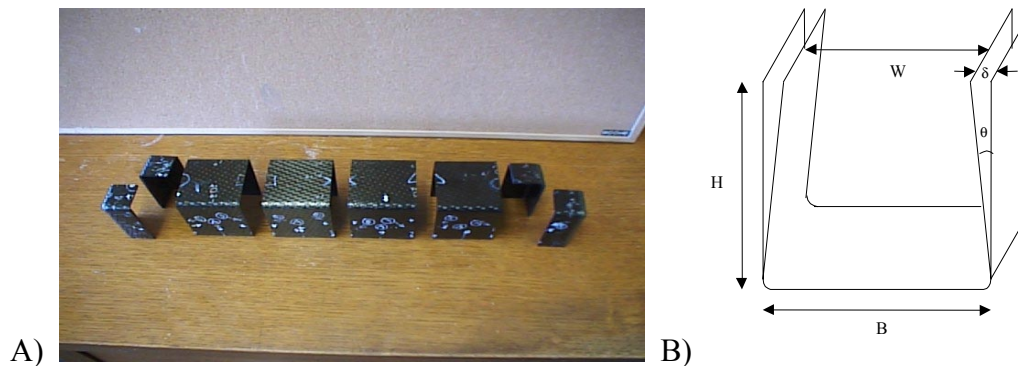


Figure 4. A) Sectioned rib, B) Definition of section geometry and spring-in.

The flange-to-flange distance, W , was measured at stations 1, 3, 5, 7, and 9. The measurements were repeated ten times and the average distance was calculated. The flange height, H , was measured at stations 1, 3, 5, 7, and 9. Data were taken from both flanges at every station and the average height was calculated. The web width, B , was measured at each station. The measurements were repeated 5 times. Figure 5 shows how the measurements were taken.



Figure 5. Measurement of: A) section height, H , B) flange-to-flange distance, W , and C) web width, B , on a sectioned rib.

2.3 Measurement Results The spring-in, δ , and spring-in angle, θ , (Figure 4B) were calculated from the measurements as follows:

$$\delta = (W - B)/2 \quad (1)$$

$$\theta = \tan^{-1}(\delta/H) \quad (2)$$

This assumes that the spring-in is the same for both flanges. The measured spring-in angle, θ , is shown in Figure 6, before and after sectioning for the five measured parts.

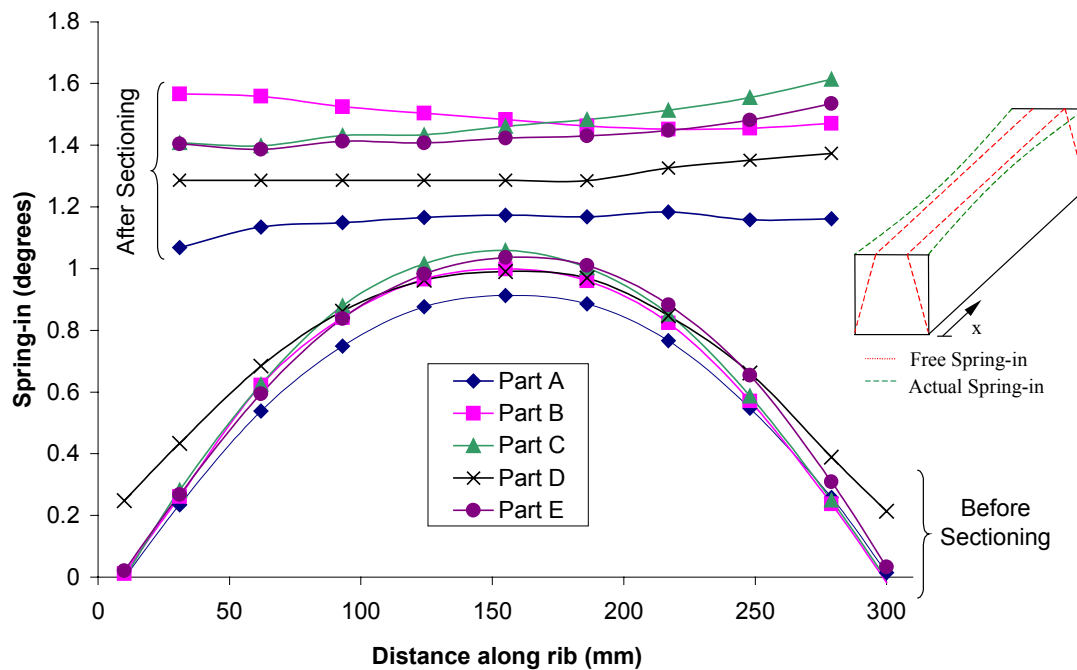


Figure 6. Measured spring-in angle, θ , before and after sectioning.

The figure shows that before sectioning, the spring-in varies in a parabolic fashion along the length of the rib, because of the constraint of the ends. After sectioning, however, the spring-in is virtually constant along the length of the rib, showing that each cross-section deforms in the same manner when the edge constraint is removed. The figure also shows that there is significant

variation in the spring-in between parts, especially after sectioning. Despite the variability in the data, there is a trend where the magnitude of the free spring-in, after sectioning, correlates with the constrained spring-in, before sectioning. This is clearly seen in the case of Part A, which has the lowest spring-in both in the free and in the constrained state.

3. MODELLING

3.1 COMPRO 2D Results A finite element model of a rib section was created in COMPRO to calculate the free spring-in. Since there is no materials database available for the cure kinetics, modulus development, cure shrinkage, and thermal expansion for the AS4/977-3 material, properties of a similar prepreg system, Hexcel Style 3K-70-PW F593, were used in the model. The model predicted a flange spring-in of 1.6° , about 15% higher than the average measured value of 1.4° .

3.2 3D Predictions To test and validate the transfer approach for the studied rib, the following approach was taken (Figure 7):

1. A 3D finite element model of the rib was created in ANSYS using orthotropic shell elements. The rib was modeled with its flanges uniformly sprung in, with the same spring-in as the average measured on the sectioned ribs, 1.4° , (Figure 6). Since the measured and predicted free spring-in was close but not correct due to the lack of material properties for the process model, the measured spring-in was used in the analysis. At this stage the structure is stress free and the vertical edges of the rib do not match up (Figure 7).
2. The ends of the long flanges were then displaced to match up with the edges of the ends of the rib. The 3D rib was modeled as an elastic fully cured composite.
3. With all edges connected, the finite element program calculated the 3D shape of the rib.

Because the properties of the AS4/977-3 material were not known at the time of modeling, the properties of Hexcel Style 3K-70-PW F593, was used in the 3D shell model.

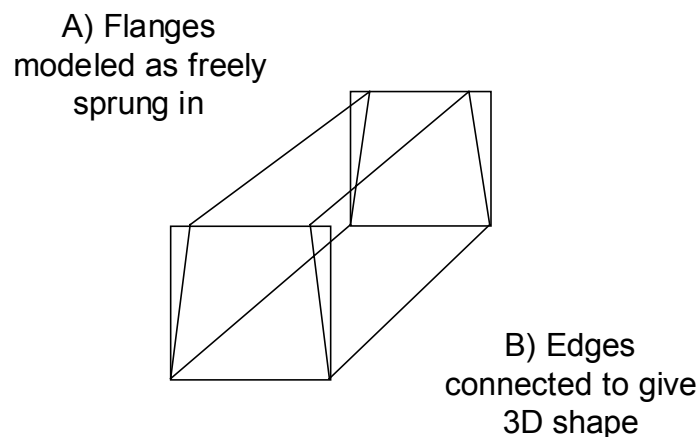


Figure 7. Schematic of 3D shell model.

3.3 Comparison of Measured Spring-in and 3D Shell Model Predictions Figure 8 shows a comparison between predicted and average measured and spring-in using the approach described above. The shape of the spring-in angle vs. distance along rib curve is predicted correctly and the magnitude is off by less than 0.1°. Note that these predictions are based on a measured free spring-in of the sections rather than a predicted value as would typically have been used using this approach. If the predicted free spring-in of 1.6° were used in the model instead, the 3D predictions would increase by about 15% and cause the discrepancy between model and measurements to be slightly larger than that shown in Figure 8.

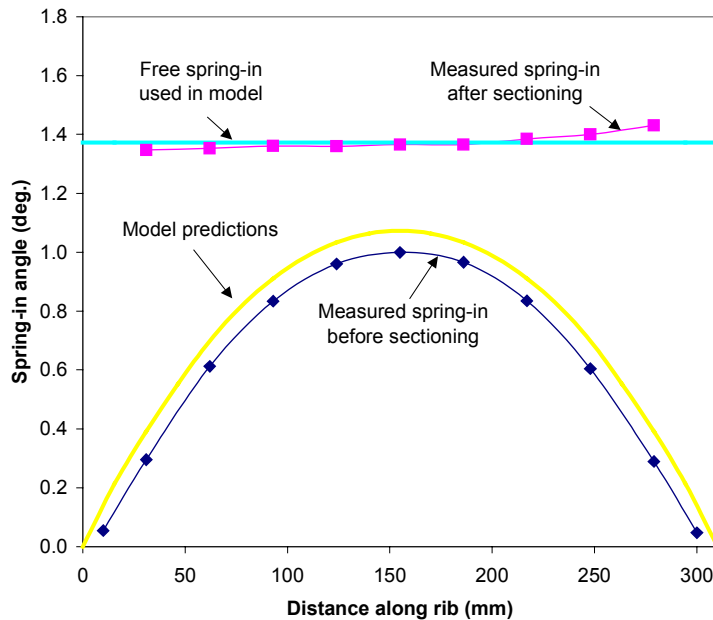


Figure 8. Comparison of average measured and predicted flange spring-in.

4. DISCUSSION AND CONCLUSIONS

The most important finding in this study is that all cross-sections of the rib have virtually the same process induced deformation (spring-in) when the ends of the rib are removed. This means that a 2D cross-sectional analysis of this problem is adequate. Furthermore, it was demonstrated that by using the information of the cross-sectional behaviour together with a simple 3D-shell model, the behaviour of the whole rib could be accurately predicted.

Although the rib studied here is representative of many composite shell structures in the aerospace industry, there will be parts where the stress build-up in the third dimension significantly affects the stresses in individual sections of the part. In such cases the approach presented here will be less accurate, perhaps to the extent of not being applicable.

5. ACKNOWLEDGEMENTS

We thank The United States Air Force Research Laboratory, Materials & Manufacturing Technology Directorate, Wright Patterson Air Force Base, Ohio, USA, for funding for the work, and our contract manager Roger Gerzeski for his effort in leading and coordinating the

“Processing for Dimensional Control” project (US Air Force contract #: F33615-97-C-5006). We also thank Jackie Lee, Amir Osooley and Robert Courdji at the UBC Composites Group for their help with experiments and modelling work, and John Griffith at Boeing St. Louis for providing the ribs.

6. REFERENCES

1. H.T. Hahn and N.J. Pagano, Curing Stresses in Composite Laminates, *J. of Composite Materials*, **9**, 91-108 (1975).
2. R. Davé, J.L. Kardos and M.P. Dudukovic, Process Modeling of Thermosetting Matrix Composites: A Guide for Autoclave Cure Cycle Selection, Proceedings of the American Society for Composites, 1st Technical Conference, 137-153 (1986).
3. A.R. Mallow, F.R. Muncaster and F.C. Campbell, Science Based Cure Model for Composites, Proceedings of the American Society for Composites, Third Technical Conference, 171-186 (1986).
4. T.A. Bogetti and J.W. Gillespie Jr., Process-Induced Stress and Deformation in Thick-Section Thermoset Composite Laminates, *J. of Composite Materials*, **26**, **5**, 626-660 (1992).
5. T.A. Bogetti and J.W. Gillespie Jr., Two-Dimensional Cure Simulation of Thick Thermosetting Composites, *J. of Composite Materials*, **25**, **3**, 239-273 (1991).
6. A.C. Loos and G.S. Springer, Curing of Epoxy Matrix, *J. of Composite Materials*, **17**, **2**, 135-169 (1983).
7. J.M. Kenny, Integration of Process Models with Control and Optimization of Polymer Composites Fabrication, Proceedings of the Third Conference on Computer Aided Design in Composite Materials Technology, 530-544 (1992).
8. S.R. White and H.T. Hahn, Process Modeling of Composite Materials: Residual Stress Development during Cure. Part I. Model Formulation, *J. of Composite Materials*, **26**, **16**, 2402-2422 (1992).
9. P. Hubert, R. Vaziri, and A. Poursartip “A Two Dimensional Flow Model for the Process Simulation of Complex Shape Composite Laminates”, to appear in *International Journal of Numerical Methods in Engineering* (1998).
10. J. Johnston, R. Vaziri, and A. Poursartip “A plane strain model for process-induced residual deformation of complex shaped composite laminates”, paper submitted to *Journal of Composite Materials* (1998).
11. K. Nelson, M. Wilenski, A. Poursartip, and G. Fernlund “Processing for dimensional control”, 44th International SAMPE Symposium and Exhibition, Long Beach, California, May 23-27 (1999), pp. 1732-1743.
12. G. Fernlund, A. Poursartip, K. Nelson, M. Wilenski, and Frederick Swanstrom “Process modeling for dimensional control – sensitivity analysis of a composite spar process”, 44th International SAMPE Symposium and Exhibition, Long Beach, California, May 23-27 (1999), pp. 1744-1755.
13. A. Johnston, P. Hubert, K. Nelson, and A. Poursartip, Finite element analysis of autoclave processing of large composite structures using a substructuring technique, 28th International SAMPE Technical Conference, November 4-7, 1996, pp. 734-744